DOI: https://doi.org/10.52756/10.52756/ijerr.2023.v31spl.002 *Int. J. Exp. Res. Rev.*, **Special Vol. 31: 12-22 (2023)**

Original Article | Peer Reviewed | Open Access

International Journal of Experimental Research and Review (IJERR)
© Copyright by International Academic Publishing House (IAPH)
ISSN: 2455-4855 (Online)
www.iaph.in

Diagnosing and categorizing of pulmonary diseases using Deep learning conventional Neural network

N. Sudhir Reddy* and V. Khanaa

Department of Computer Science and Engineering, Bharath Institute of Higher Education and Research (BIHER), Chennai, Tamil Nadu, India

E-mail/Orcid Id:

NSR, nsudhir771@gmail.com, https://orcid.org/0009-0004-1132-6863; *VK*, drvkannan62@bharathuniv.ac.in, https://orcid.org/0000-0002-2509-1549

Article History:

Received: 22nd Mar, 2023
Accepted: 13th May, 2023
Published: 30thJul., 2023

Keywords:
Hybrid fuzzy morphological, region of interest, NLTF, laplacian pyramid decomposition

Abstract: Lung cancer is one of the major illnesses that contribute to millions of fatalities worldwide. Numerous deaths could be saved through the early identification and categorization of lung cancers. However, with traditional approaches, classification accuracy cannot be produced. To detect and classify lung diseases, a deep learning convolutional neural network model has been developed. LDDC, the customized local trilateral filter, is used for pre-processing the lung images from computing tomography for non-local trilateral filters. The region of interest for lung cancer was successfully restricted throughout the segmentation of the disease using hybrid fuzzy morphological procedures. To extract the deep seismic features, the Laplacian pyramid decomposition method was utilized for the segmented image. This paper covers an overall analysis of non-local trilateral filter Processing, hybrid fuzzy morphological techniques and analysis of patient and disease characteristics of LIDR- IDRI and FDA data of Group A (no co-AGA), P-value, Multi-mut Patient, Group B (with a co-AGA).

Introduction

Numerous millions of humans worldwide are afflicted with lung cancer, one of the most serious types of cancer. Pulmonary disease incidence recently increased abnormally as a consequence of the COVID-19 outbreak. Furthermore, there is a clear link between COVID-19 and lung cancer (Sharif, 2020), as COVID-19 is more likely to affect people who have lung cancer. Numerous investigations have been conducted in the crucial research area of lung cancer segmentation and classification (Shakeel et al., 2022; Asuntha and Andy, 2020). Thus, a billion lives can be saved through the early identification and categorization of lung cancers. Conventional CAD systems (Yu, 2020) operate lacking intelligence at all using simple computational image processing techniques, which leads to subpar segmentation and categorization performance. Recently CAD systems have been created using AI prototypes like machine learning and deep learning models (Saha and Yadav, 2023). However, due to their high computational complexity and poor classification performance, traditional machine-learning techniques are suffering. Consequently, deep learning models must be used in CAD systems rather than machine learning techniques.

The motivation behind deep learning conventional neural networks for the diagnosis and classification of lung conditions stems from a desire for reliable, effective, and readily obtainable tools for diagnosis. the requirement for precise, effective, and easily available diagnostic tools in bright of rising disease prevalence, complex disease presentations, a lack of knowledge, and developments in medical imaging technology. By offering credible, accurate assessments, such models offer the possibility to revolutionize the identification of pulmonary diseases, thereby enhancing the treatment of patients and prognosis.

For the purpose of creating a dataset over the process of segmentation, we used the DLCNN (Bhatia et al., 2019) over lung image categorization as well as the morphological chart cut method for border generation on

***Corresponding Author:** nsudhir771@gmail.com

the generated images. The data set used for initial training did not require any manually performed labeling activities to be completed. Artificial intelligence and medical imaging techniques are combined in order to create CADs (Schwyzer, 2018) and for pulmonary segmentation and categorization. Lung membranes segmentation is used as an initial processing stage in lung CT image processing, which is very beneficial in the area of lung disease in particular. The final CT image preparation is directly impacted by the pre-processing (Lakshmanaprabu, 2019) procedures. Therefore, developing quicker and more precise segmentation methods for lung CT scans is an intriguing issue that merits research due to its urgent, practical requirement and clinical importance. Numerous lung division methods are being researched, and a small number of traditional methods incorporate threshold region-development strategies (Ardila, 2019). However, the process is laborious and costly, and the outcomes are not very encouraging. As a result, it is still regarded as unexplored territory.

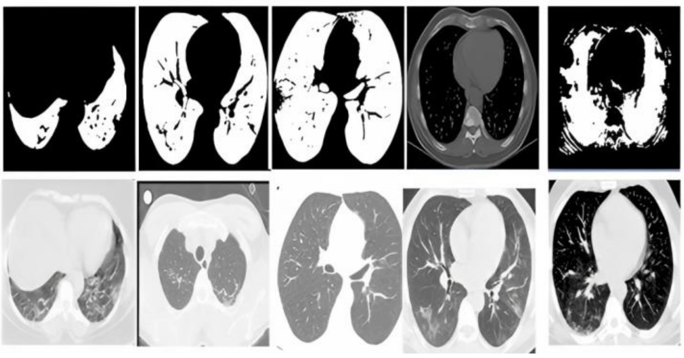

Figure 1. CT scans Image of Processing data along with HFM Image

Since the projected proportions of the lung borders have been the same with those of the passageway and bronchus region, the segmentation, even though being finished swiftly, is of poor quality. A basic image-segmentation method that depends on the CT scans area is deep learning (Riquelme and Moulay, 2020). It can rapidly and effectively divide the borders of the interstitial lung. Although this method works, it takes a lot of effort, and the creation of the model is delicate to boundaries. Most segmentation of lung approaches in use today are hybrid systems that combine an edge-respecting approach with unexpected evolution and other retrieval processes. Additionally, a number of examinations are carried out in the event of a lung infection based on the organization of the pulmonary parenchyma. The novelty of the work is shown through following steps:

a) The initial phases, NLTF is used to improve the cancer spot and eliminate various kinds of noise regarding pulmonary CT images.
b) Next, structural creating and closing-based fuzzy processes are used to pinpoint the ROI for cancer using HFM-based segmentation.
c) The illness-specific characteristics are obtained using the lung cancer prediction process applied to segmented images and GOA is utilized for obtaining the deeper seismic features.
d) In the end, a DLCNN models conducted training and evaluation procedures using the features obtained and diagnoses benign and malignant cancers of the lungs.

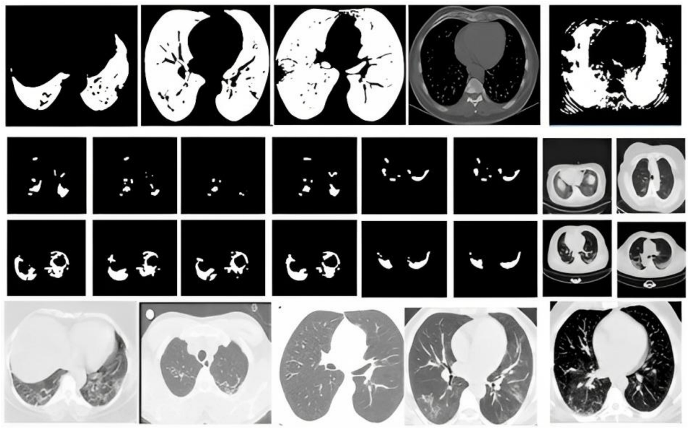

Figure 2. Collection of Image processing LDDS –net and HFM dataset after processing

The remainder of the article was provided by: Section 2 addresses with the related work in the issue statement. The thorough analysis of the proposed LDDS-Net is covered in Section 3. The fourth section discusses results and discussion contrasts them with traditional methods. The article's potential future improvements are covered in Section 5.

Methods

There are numerous medical imaging modalities existing, each with a distinct set of advantages. Additionally, this advances the use of processing techniques. Multi-scale computed tomography (CT) categorization is a common approach among the scientific field. Using this method, multiple medical photographs are combined into one image. It is several investigations (Chaunzwa et al., 2021) have been carried out in CT scan-based cancer of the lungs identification with classification. The research illustrates how automated learning approaches had decreased their categorization exactness and produced unconstitutional classification. Several evolutionary techniques for lung segmentation with indicate filtering-based preparation operations were provided by the authors in (Lee et al.,

DOI: https://doi.org/10.52756/10.52756/ijerr.2023.v31spl.002

2020). Several computations with enhanced accuracy were applied to the beforehand processed CT images with the goal of enhancing their general quality. MATLAB was used to test the outcomes to make sure practical findings for 20 sample lung scans. This strategy's computational complexity (Toğaçar et al., 2020) continues to be lowered. Additionally, the authors (Bhandary, 2020) focused on lung tumor analysis using enhanced median filter-based blurring via thresholds segmentation, improved the precision of the preparing by Gaussian filter (Avanzo et al., 2020) for these images in this study, which resulted in the creation of an algorithm. This perform has a great deal greater sensibility, particularity, exactness as well as preciseness than before methods, with a decreased proportion of false positive aspects. Pyramid-based classification and other multi-scale image segmentation and classification techniques (Huang et al., 2019) are currently in use, along with a number of other multistage image classification algorithms. The changing parameters provide pertinent information for each of the strategies outlined (Singh and Gupta, 2019). The details of the segment are collectively as a result of measuring the parameters as well as detailed pertinent information that data collected along with the segmented CT scan. The fundamental morphological approaches used by the authors (Nasrullah et al., 2019) for segmenting CT images produced an impressive performance for caring for diseases that failed to segment cruel diseases. The morphological theory is being used more frequently in image segmentation uses like adaptive threshold (Jakimovski and Davcev, 2019), noising, resolution processing and segmentation. The authors (Sarkar et al., 2019) highlighted the potential of optimized machine learning techniques in predicting occupational accidents. By leveraging feature selection, parameter tuning, and model ensemble techniques, the study demonstrates improved predictive accuracy compared to traditional approaches. An objective-subjective weighted method for minimizing inconsistency in multi-criteria decision-making, ublished in the journal Computers & Industrial Engineering introduces a novel method (Paramanik et al., 2022) for handling inconsistency in decision-making processes involving multiple criteria. The study's results demonstrate the proposed approach's effectiveness in predicting injury severity (Sarkar et al., 2020). The machine learning models trained on the combined proactive and reactive data outperform models trained solely on reactive data. The combination of oversampling and under sampling techniques helps mitigate the class imbalance problem and improves the overall performance of the models. The paper (Pramanik et al., 2021) discusses the technical aspects of the system, including the algorithms and methodologies used for event detection. It explores various computer vision techniques, such as object detection, tracking, and motion analysis, to identify relevant objects and behaviors in the video streams. The paper (Sarkar et al., 2021) presented a case study focused on incident analysis in a steel plant using text mining-based association rule mining techniques. The study is based on the research effort iofn (Bag et al., 2023) which emphasizeded the multiple important processes. Driving data, which may include information from GPS sensors, accelerometers, and other pertinent sources, is first used to extract the spatio-temporal properties. Second, the haviorsurs and decision-making patterns of the driver are examined in order to derive driver praxeological traits. This paper (Dey et al., 2023) examines how supply chain management practices can rate technologies based on artificial intelligence (AI), including machine learning, forecasting, and optimisation algorithms. The results of the research (Das and Sarkar, 2022) showed how effective AI-driven methodologies are. The use of machine learning algorithms enables the recognition of key variables affecting the efficiency and adaptability of the entire supply chain.

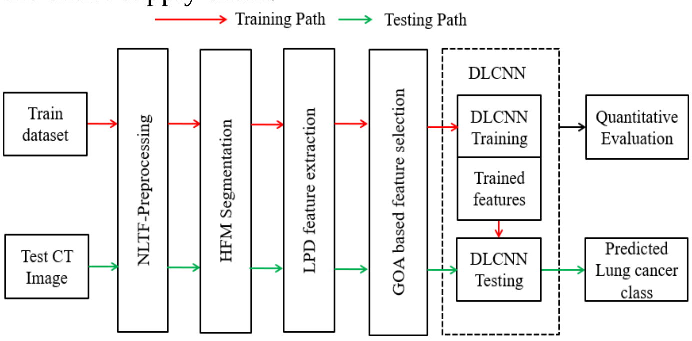

Figure 3. Flow diagram of processing the medical data for training and testing purposes.

The Figure 3 represents the training and processing of data and their framework of artificial intelligence prototypes. The SR theory has paid attention to a lot of recent work happened in in the field of image processing and especially in the perspective of image categorization (Masood, 2018). Recently the (FCM) Fuzzy c-means clustering (Wang, 2019) and (MOTSU) Modified OTSU (Ozdemir and Gleeson, 2018) can be used to create dictionaries for conventional SR algorithms when segmenting lung images. But when it comes to classifying CT scans, conventional SR algorithms with set vocabulary have a number of drawbacks. SVM models for image classification and deposing were suggested in (Ruan, 2022), and they can create an adaptive compacted directory for the classification of CT

DOI: https://doi.org/10.52756/10.52756/ijerr.2023.v31spl.002

Table 1. LDDS Algorithm for Feature Extraction, Segmentation and Data Processing

Input: Test CT image, LIDC-IDRI dataset **Performance measures:** Image Pre-processing, Image segmentation and metrics classification. **Output:** Image segmentation and classification of Lung Cancer classes.	
Step 1	Applying the NLTF pre-processing for noise reduction and optimization of CT scans to the LIDC-IDRI dataset used for training.
Step 2	Use HFM segmentation to localize the area affected by lung cancer.
Step 3	Apply LPD to the results of the HFM segmentation to extract the particular details of the disease.
Step 4	Use a bio-optimization strategy based on GOA to choose the best characteristics.
Step 5	Execute training of DLCNN-based data, extract the features as well as train it and evaluate the efficiency of classification and segmentation.
Step 6	Take data from the test CT Image and carry out steps 1 through 5 again to extract the new image featuring.
Step 7:	DLCNN techniques use testing purposes and use for prediction to identify lung cancer illnesses.
Step 8:	Assess the measures for the pre-processing of image, segmentation and Image classification and evaluate them to the state-of-the-art.

images and combine the images collected from various sources. Scholars claim that this approach may be employed to add SR to customized spatial frequency along with k-means clustering (KMC), which is used for pulmonary segmentation of images, as well as the basic idea of an adaptive decision dictionary. The training and processing of data and their framework of artificial intelligence prototypes are defined in the diagram. The two unnecessary wavelet modifications as further language Transform (LT) depending support vector machine (SVM) (Punithavathy et al., 2019) as well as Redundant Independent Transform (R-DIT) centered convolution neural networks neural network (CNN) (Polat and Homay, 2019) utilized for lung cancer categorization look at with multi-view healthcare imaging. They found that the shift-invariance of the R-DIT method can be used to quickly and accurately create classifications for CT scans using their proposed method. A technique called pyramid transformation may be used to accomplish the classification of numerous CT scan views (Thakur et al., 2020). This method was initially presented, but it was rapidly adopted and widely used in a range of uses, such as CT scan division, data compression as well as machine learning (Park et al., 2019). An extensive list of essential features (Ozdemir et al., 2019) could be extracted from the segmented CT scans thanks to the author's (Masood et al., 2019) presentation of the combined ResNet51 method for multiple classes of lung cancer classification. The authors suggested Laplacian Pyramids Region Mosaicking for extraction of features with GoogleNet (Qin et al., 2020; Chao et al., 2021) as a technique for combining CT images obtained by microscopes, but it was discovered that it was noise-prone. When the extensive underlying features of the image were revealed, the laplacian pyramid technique with combined averaging was elective, which produced a significant improvement in the output.

Proposed Work

The suggested framework carries out four main activities, including NLTF-based preliminary processing, LPD-based feature extraction, HFM segmentation, GOA-based feature selection and DLCNN categorization, which are all covered in depth in this subsection. The suggested LDDS-Net architecture is shown in Figure 1, and the suggested LDDS-Net algorithm is shown in Table 1.

Table 2. NLTF Model Information

Layer	Type	Input	Kernel	Output
1	Convolution	28×28×1	5×5	24×24×32
2	Max pooling	24×24×32	2×2	12×12×64
3	Convolution	12×12×64	5×5	8×8×64
4	Max pooling	8×8×64	2×2	4×4×64
5	Fully connected	4×4×64	4×4	512×1
6	Fully connected	512×1	1×1	2×1
7	Softmax	2×1	N/A	Result

NLTF Processing

The context of Natural language image processes and computer visualization purpose is to resolve high disparity image and marlin image, the trilateral filter used for a nonlinearly single-pass filter in order to keep the border of thinning and discernible detail for N-

DOI: https://doi.org/10.52756/10.52756/ijerr.2023.v31spl.002

dimensional messaging. The trilateral filter inserts local image statistics into the BF to detect pixels that are noisy in random pictures influenced by impulse noise. The brightness differential among a midpoint pixel and it's nearest equivalent neighbors is expressed as an NLTF number. The trilateral filtration is ideal for minimizing Gaussian noise, regular noisy impulses, and mixture. A pipeline design that uses trilateral noisy filters to solve the complexity issue with conventional trilateral filtration. The main challenge in applying such a powerful noisy filtration to real-time imagery systems was its extremely high temporal complexity. The Figure 2, approached the computation of NLTF is done bitwise and the evaluation of the exponential equation is done partially employing linear estimates. Trilateral filters were used to create an adaptive trilateral filter that made use of the NLTF and the Rank Ordered Logarithmic Difference statistic. The NLTF is already a good statistic for measuring pulse noise in images, but some bruising pixels may have intensity values that are similar to those of their adjacent pixels for pulse noise with randomly valued values. The pixel NLTF won't be big enough, in this case, to distinguish between it and the noise-free pixels. The logarithmic function is known as the ROLD function to improve the input picture.

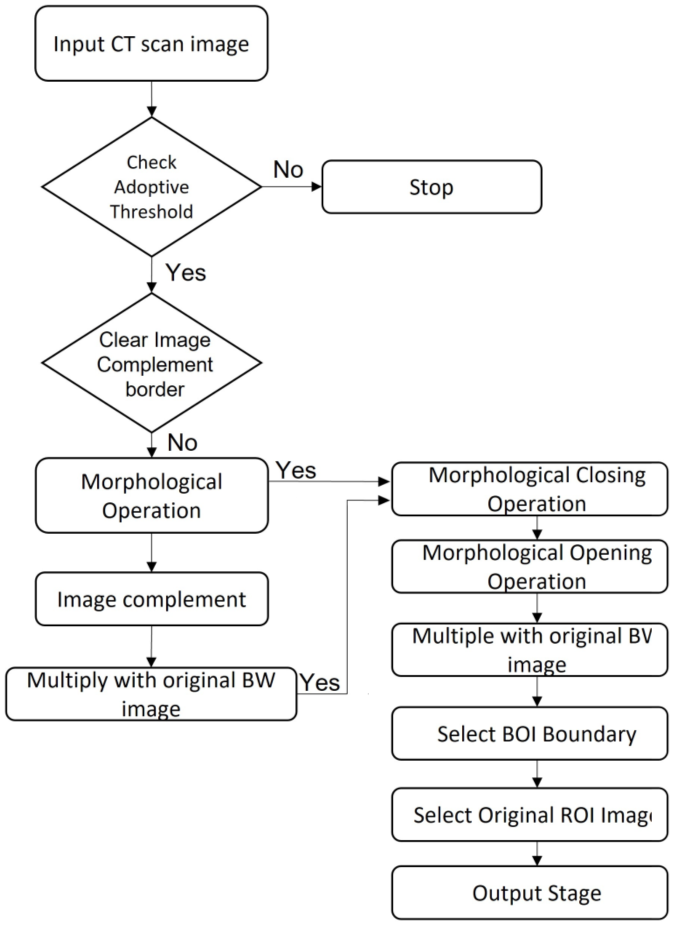

Figure 4. Flowchart for Segmentation Recommendation for NLTF

Numerous medical computer vision applications used for the classification of various types of lung cancer, make extensive use of the NLTF models. This method of comprehension has lately attracted a lot of attention due to its success. NLTFs have the advantages of being much easier to learn and having fewer characteristics than fully connected networks. The NLTF Model Information for different types is shown in Table 2.

Table 2. NLTF Model Information

Layer	Type	Input	Kernel	Output
1	Convolution	28×28×1	5×5	24×24×32
2	Max pooling	24×24×32	2×2	12×12×64
3	Convolution	12×12×64	5×5	8×8×64
4	Max pooling	8×8×64	2×2	4×4×64
5	Fully connected	4×4×64	4×4	512×1
6	Fully connected	512×1	1×1	2×1
7	Softmax	2×1	N/A	Result

The maximum pooling layer would then select the best deal from each kernel to reduce the number of features. In order to achieve the best results with the least quantity of computational work, multiple iterations of the convolution and max-pooling layers are used. Additionally, while mapping input to output features, a completely connected layer maintains all neurons and their interconnections. Finally, the softmax classifier is always used to distinguish between the compassionate and malignant classes.

HFM Segmentation

When pulmonary parenchyma splitting is carried out, it is quite helpful in identifying and evaluating neighboring lesions, but it is only efficient if specific methods and frames are applied. The creation of lung modules from CT picture succession is used in the CAD organization and the pulmonary parenchyma segmentation is a crucial pre-processing stage.

When creating the LDDS-Net, an efficient thresholds approach was used to simplify lung segmentation in order to speed up computation while decreasing complexity. Using experiments and data analysis, the method was evaluated on a numeral of CT scans obtained from the LIDC-IDRI.

Result and Discussion

This portion provides a thorough analysis of simulation results along with comparisons using cutting-edge techniques. The same dataset was used to implement the suggested LDDC-Net and traditional

DOI: https://doi.org/10.52756/10.52756/ijerr.2023.v31spl.002

methods. To assess the superiority of each technique, the study suggested that LDDC-Net was also performed well for image processing.

The table 3 highlight the new dataset collection of 1018 set in different age group along with classification in eight imaging along with 12 criteria measurement for identification of lung Pulmonary. The dataset covered the

Table 3. The individual report of patient and disease distinctiveness of LIDR- IDRI and FDA data (groups A and B respectively)

Parameters	multi-mut patients N(54)	Group A (co-AGA) N (21)	Group B (co-AGA) N (32)	p-value
Average Age Median (Years)	71 (38-85)	76 (45-85)	68 (34-80)	0.300
Sex - men	28 (50.6%)	18 (68.7%)	12 (34.0%)	0.021
Histology	----	----	----	<0.001
Adenosquamous	2 (2.1%)	1 (5.2%)	0	----
NSCLC	2 (3.5%)	0	3 (6.3%)	0.860
Squamous cell	13 (22.8%)	9 (39.6%)	4 (7.6%)	----
Smoking status-Before	14 (24.6%)	4 (18.2%)	10 (28.6%)	----
Smoking status-Current	13 (22.8%)	5 (22.7%)	8 (22.9%)	----
Smoking status-Former	23 (40.4%)	9 (40.9%)	14 (40.0%)	----
PDL1 expression (<1%)	12 (19.5%)	6 (24.3%)	8 (23.0%)	0.278
PDL1 expression (1–49%)	8 (18.6%)	5 (25.7%)	3 (10.4%)	0.278
PDL1 expression (>49%)	14 (29.4%)	4 (14.2%)	11 (28.3%)	0.278
MR	1 (1.8%)	2 (3.8%)	0 (0.0%)	----
NSCLC	2 (3.5%)	0 (0.3%)	2 (5.7%)	----
Squamous cell	11 (23.4%)	9 (43.4%)	3 (8.6%)	----
NE Large cell	2 (2.2%)	1 (4.5%)	0 (0%)	----

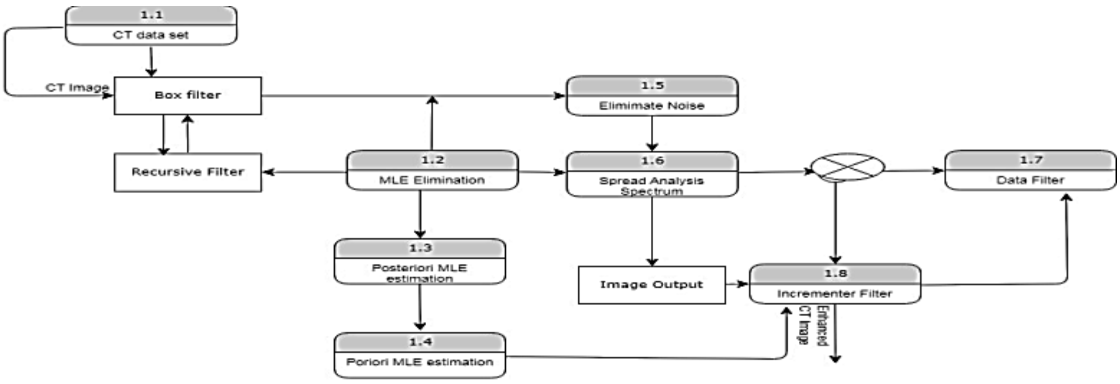

Figure 5. HFM processing diagram

Dataset

The Pulmonary Imagery Data Consortium (LIDC-IDRI) image library consists of thoracic CT pictures for diagnostic and screening purposes with highlighted and labelled lesions. These libraries are a global web-based platform for the creation, instruction and assessment of CAD systems for lung cancer recognition and detection. The following public-private enterprise organization uses the data of the National Disease Institute (NCI) and other foundations like the National Institutes of Health (FNIH) as well as the Food and Drug Administration (FDA) through active engagement, illustrates the achievement of a relationship founded on a consensus-based procedure.

patient and disease characteristics for each group along with the possibility of the chance to lung Pulmonary. The table 3 highlighted the dataset collection of 1018 sets in different age groups along with classify in eight imaging along with 12 criteria measurements for identification of lung Pulmonary. The dataset covered the patient and disease characteristics for each group along with the possibility of the chance to lung Pulmonary.

The CT scan picture focused on bold. PD – Progressive Disease, NA for Not Assessed, MR – Mixed Response, NSCLC represents Non-Small Cell Lung Carcinoma, NE – Neuroendocrine, SD – Stable Disease, IO – Immunotherapy, PR – Partial Response. The Table 4 also denotes the mutation ratio of each age group for identification of Group A and Group which age group (28-92), Group (no co-AGA), which age group (48–90) and non-multi-mut, non-AGA patients of Group C with age group (27–88) along with different Parameters like Average Age Median(Years), Smoking status, Large cell NE, Adenosquamous, Histology, Squamous cell. The insignificant p values are highlighted in bold. NOS – not otherwise specified.

multi-mut patients, Group A (no-coAGA) with associated P-value. The Unknown data reflected that not supposed to reflect anything during that time but future activities depend on P-value of PD, PR, NE value. The Pulmonary Imagery Data Consortium (LIDC-IDRI) image library consists of thoracic CT pictures for diagnostic and screening purposes with highlighted and labelled lesions. It is a global web-based platform for the creation, instruction, and evaluation of CAD methods for lung cancer diagnosis and detection. The Group B (with a Co-AGA) has high possibility of deducting the cancer as compared to mutli-mut patients, Group A (no-coAGA). The P- value of Group B is reflected very high.

Table 4. Individuals suffering from the PIK3CA variant who do not additionally have a co-actionable genetic alteration (AGA), or group A, as well as group C, have similar baseline patients and illness features

Parameters A	Group A+GroupC		Group (co-AGA)		Group C (non-multi-mut , non-AGA patients)		p-value
	N-240	%	N-14	%	N-289	%	
Average Age Median(Years)	65	(28–92)	68	(48–90)	59	(27–88)	0.029
Sex (men)	247	676%	12	68.7%	229	59.2%	0.241
Smoking status-Before	54	16.2%	2	16.1%	56	16.2%	0.245
Smoking status-Current	121	33.7%	8	29.8%	106	33.8%	0.245
Smoking status-Former	168	47.7%	7	44.5%	156	48.0%	0.245
Smoking status-NA	8	2.4%	1	9.9%	5	2.0%	0.245
Squamous cell	102	34.1%	9	49.6%	89	28.8%	----
Histology							0.013
Adeno squamous	1	0.002%	1	6.1%	0	0%	----
Large cell NE	7	1.4%	0	0%	7	0.9%	----

Analysis

The initial processing and segmentation-based visible subjective evaluation is displayed in this section. The figure 6 displays the results of the NLTF pre-processing, which successfully reduced the various backdrop noises and emphasized the cancer-reflection area. Additionally, NLTF enhances the spatial and consistency characteristics of each pixel. The segmented output images from the HFM method are shown in graph. The cancer region is precisely segmented by the suggested HFM technique. The figure 6 highlighted the Overall analysis of Group A with effectiveness of the lung cancer diseases. The value 3.63, 38.6 and 47.6 with repeated value supposes to highlight for Pulmonary and Lung Cancer. The crossover of yellow and red graph suggested the Lagecell NE, Histology mutation of Middele Age 40-45.

The figure 7 covered the cumulative analysis of NLTF spatial and texture characteristics of each pixel. The segmented output images from the HFM method along with different parameters like Group B (with a Co AGA),

The Fig 8 shows the CT scan picture that signifies p values tinted as bold. IO – Immunotherapy, NA represents Not Assessed, MR – Mixed Response, NSCLC denotes Non Small Cell Lung Carcinoma, PR – Partial Response, SD – Stable Disease, PD – Progressive Disease, NE – Neuroendocrine. The Table 3 also denotes the mutation ratio of each age group for identification of Group A and Group which age group (28-92), Group (no co-AGA) which age group (48–90) and non-multi-mut, non-AGA patients of Group C with age group (27–88) along with different Parameters like Average Age Median (Years), Smoking status, Large cell NE, Adenosquamous, Histology, Squamous cell. The respective p-values are represented as bold. The NA represents Not Assessed, NSCLC represents Non-Small Cell Lung Carcinoma

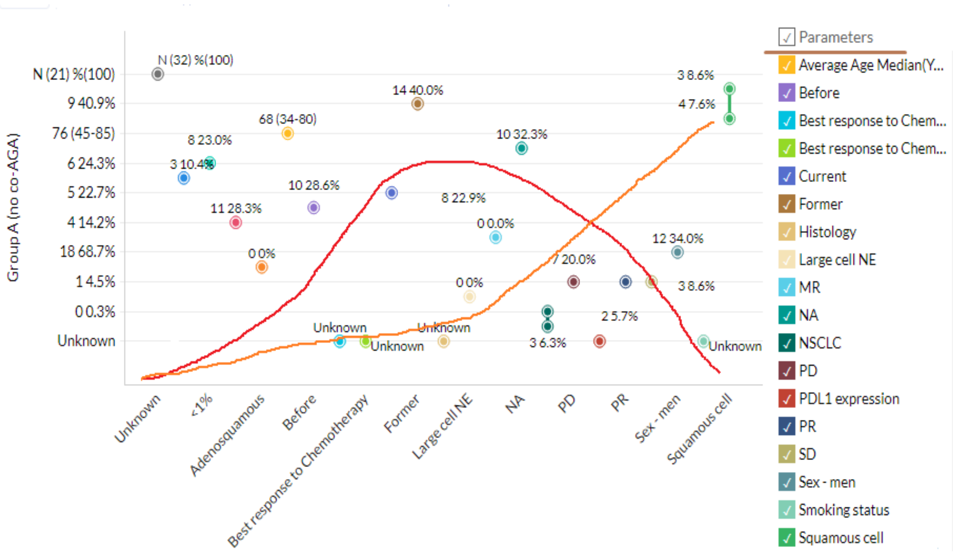

Figure 6. Group A (no co –AGA) with effectiveness of the lung cancer diseases

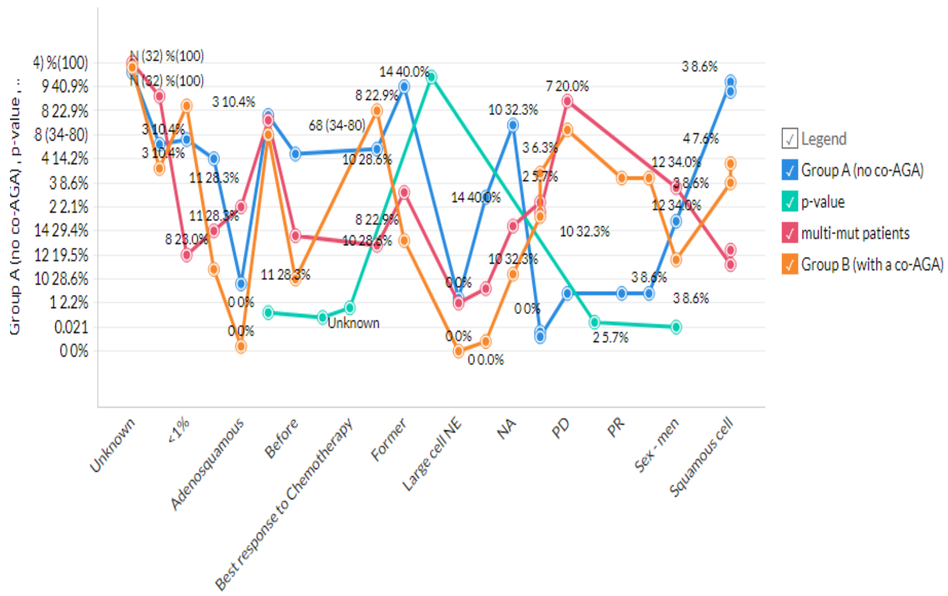

Figure 6. NTLF and HFM analysis of Group A(no co-AGA), P-value, Multi-mut Patient, Group B (co-AGA)

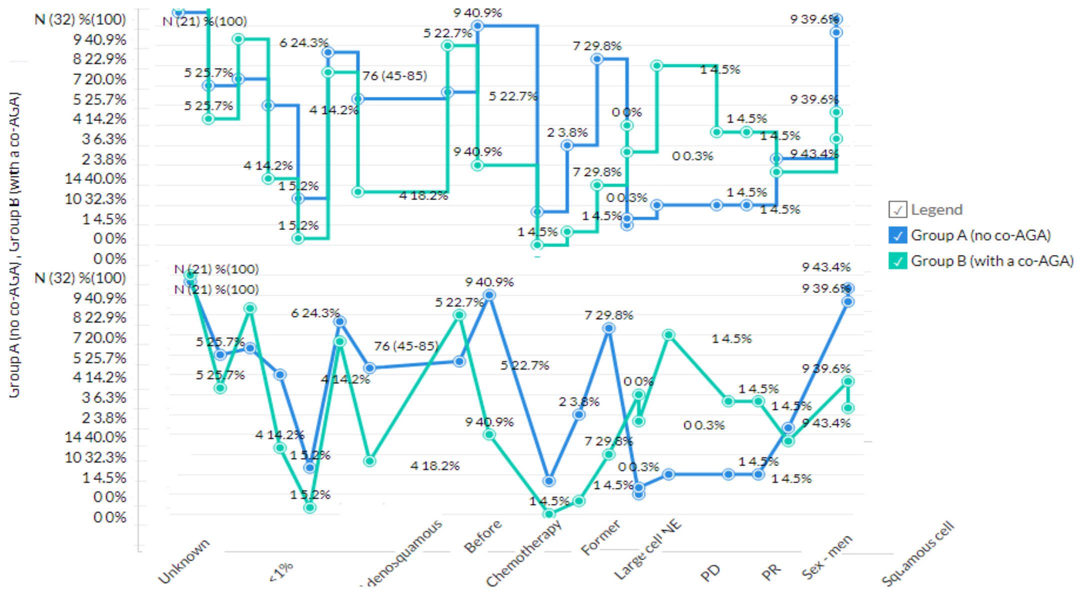

Figure 8. Analysis of N(32)% 100 for Group A and Group B

and NOS for not otherwise specified. A dataset collection of 1018 set in different age groups along with classified into eight imaging along with 12 criteria measurements for identification of lung Pulmonary. The dataset covered the patient and disease characteristics for each group along with the possibility of the chance to lung Pulmonary. The details mentioned in Figure 8 in below. The Analysis of N(32)% 100 for Group A and Group B cover all unknown parameter which synthesizes the possibilities of happening and un-happening condition. The comparison and performance of the projected NLTF method with conservative approaches like LDDC- Net and others will not be sure to give a proper hypothesis of lung Cancer. Furthermore, when compared with all other methods, the one recommended NLTF performed better for all measures. Evaluation of the effectiveness of preprocessing techniques is shown graphically in Figure 8.

Conclusion

The division and multiple classes categorization of lung cancers were suggested in this paper using the deep learning as well as bio-optimization dependent LDDC-Net model. NLTF was initially employed to improve the disease-affected area and reduce various noises since CT source imagery. The disease-affected area was then localized using HFM-based the segmentation process. Deep spectral features were also extracted from the segmented pictures using LPD. Additionally, the deep interdependent features with disease-specific likelihood reliant features were chosen using a bio-optimization strategy that utilized GOA. Finally, the DLCNN model was employed to accurately identify CT lung image's benign and malevolence set. The imitation findings demonstrate that comparison to the projected LDDC-Net, segmentation, preprocessing of image and classification of image performance was all significantly improved. The practical implications of using deep learning has the ability to reduce diagnostic errors, which has practical consequences for pulmonary disease diagnosis. In order to learn complicated patterns and characteristics that are suggestive of particular diseases, deep learning models can be trained on massive datasets of medical images, such as chest X-rays and CT scans. Deep learning models can provide precise and objective judgments by analyzing these photos, assisting medical practitioners in making better-informed decisions.

The theoretical standpoint, the utilization of deep learning in pulmonary disease diagnosis contributes to the advancement of medical research and knowledge. Deep learning algorithms can find intricate connections and patterns in medical imagery that can be challenging for human professionals to recognize. These models can locate subtle characteristics and relationships that can be suggestive of early-stage or uncommon lung diseases by analyzing enormous volumes of data. This information can deepen our understanding of these ailments and help us create more specialized treatment plans. The simulation's findings demonstrate that the recommended LDDC-Net achieves conventional methods in terms of pre-processing, segmentation and classification accuracy.

Conflict of Interest

The authors declare no conflict of interest.

References

Ardila, D. (2019). End-to-end lung cancer screening with three-dimensional deep learning on low-dose chest computed tomography. *Nature Medicine, 25*(6), 954-961. https://doi.org/10.1038/s41591-019-0447-x

Asuntha, A., & Andy, S. (2020). Deep learning for lung Cancer detection and classification. *Multimedia Tools and Applications, 79*(11), 7731-7762. https://doi.org/10.1007/s11042-019-08394-3

Avanzo, M., Stancanello, J., Pirrone, G., & Sartor, G. (2020). Radiomics and deep learning in lung cancer. *Strahlentherapie und Onkologie, 196*(10), 879-887. https://doi.org/10.1007/s00066-020-01625-9

Bag, S., Golder, R., Sarkar, S., & Maity, S. (2023). SENE: A novel manifold learning approach for distracted driving analysis with spatio-temporal and driver praxeological features. *Engineering Applications of Artificial Intelligence, 123*, 106332. https://doi.org/10.1016/j.engappai.2023.106332

Bhandary, A. (2020). Deep-learning framework to detect lung abnormality–A study with chest X-Ray and lung CT scan images. *Pattern Recognition Letters*, *129*, 271-278. https://doi.org/10.1016/j.patrec.2019.11.013

Bhatia, S., Yash S., & Lavika G. (2019). Lung cancer detection: a deep learning approach. *Soft Computing for Problem Solving*. J.C. Bansaletal. (eds.), Soft Computing for Problem Solving, Advancesin Intelligent Systems and Computing 817, Springer, Singapore. pp. 699-705. https://doi.org/10.1007/978-981-13-1595-4_55

Chao, H., Shan, H., Homayounieh, F., Singh, R., Khera, R. D., Guo, H., & Yan, P. (2021). Deep learning predicts cardiovascular disease risks from lung cancer screening low dose computed tomography. *Nature Communications*, *12*(1), 1-10. https://doi.org/10.1038/s41467-021-23235-4

Chaunzwa, T. L., Hosny, A., Xu, Y., Shafer, A., Diao, N., Lanuti, M., & Aerts, H. J. (2021). Deep learning classification of lung cancer histology using CT images. *Scientific Reports*, *11*(1), 1-12. https://doi.org/10.1038/s41598-021-84630-x

Das, S., & Sarkar, S. (2022). News media mining to explore speed-crash-traffic association during COVID-19. *Transportation Research Record,* 03611981221121261. https://doi.org/10.1177/03611981221121261

Dey, P., Chowdhury, S., Abadie, A., Yaroson, E. V., & Sarkar, S. (2023). Artificial Intelligence-Driven Supply Chain Resilience in Vietnamese Manufacturing Small-and Medium-Sized Enterprises. *International Journal of Production Research*, pp. 1-40. https://doi.org/10.1080/00207543.2023.2179859

Huang, P., Lin, C. T., Li, Y., Tammemagi, M. C., Brock, M. V., Atkar-Khattra, S., & Lam, S. (2019). Prediction of lung cancer risk at follow-up screening with low-dose CT: a training and validation study of a deep learning method. *The Lancet Digital Health*, *1*(7), e353-e362. https://doi.org/10.1016/s2589-7500(19)30159-1

Jakimovski, G., & Davcev, D. (2019). Using double convolution neural network for lung cancer stage detection. *Applied Sciences:* 9(3), 427. https://doi.org/10.3390/APP9030427

Kadir, T., & Gleeson, F. (2018). Lung cancer prediction using machine learning and advanced imaging techniques. *Translational Lung Cancer Research: 7*(3), 304. https://doi.org/10.21037/tlcr.2018.05.15

Lakshmanaprabu, S. K. (2019). Optimal deep learning model for classification of lung cancer on CT images. *Future Generation Computer Systems, 92*, 374-382. https://doi.org/10.1016/j.future.2018.10.009

Lee, J. H., Sun, H. Y., Park, S., Kim, H., Hwang, E. J., Goo, J. M., & Park, C. M. (2020). Performance of a deep learning algorithm compared with radiologic interpretation for lung cancer detection on chest radiographs in a health screening population. *Radiology*, *297*(3), 687-696. https://doi.org/10.1148/radiol.2020201240

Masood, A. (2018). Computer-assisted decision support system in pulmonary cancer detection and stage classification on CT images. *Journal of Biomedical Informatics, 79,* 117-128. https://doi.org/10.1016/j.jbi.2018.01.005

Masood, A., Yang, P., Sheng, B., Li, H., Li, P., Qin, J., & Feng, D. D. (2019). Cloud-based automated clinical decision support system for detection and diagnosis of lung cancer in chest CT. *IEEE Journal of Translational Engineering in Health and Medicine, 8*, 1-13. https://doi.org/10.1109%2FJTEHM.2019.2955458

Nasrullah, N., Sang, J., Alam, M. S., Mateen, M., Cai, B., & Hu, H. (2019). Automated lung nodule detection and classification using deep learning combined with multiple strategies. *Sensors*, *19*(17), 3722. https://doi.org/10.3390/s19173722

Ozdemir, O., Rebecca, L. Russell., & Andrew, A. B. (2019). A 3D probabilistic deep learning system for detection and diagnosis of lung cancer using low-dose CT scans. *IEEE Transactions on Medical Imaging, 39*(5), 1419-1429. https://doi.org/10.48550/arXiv.1902.03233

Park, S., Lee, S. M., Do, K. H., Lee, J. G., Bae, W., Park, H., & Seo, J. B. (2019). Deep learning algorithm for reducing CT slice thickness: effect on reproducibility of radiomic features in lung cancer. *Korean Journal of Radiology*, *20*(10), 1431-1440. https://doi.org/10.3348/kjr.2019.0212

Pramanik, A., Sarkar, S., & Maiti, J. (2021). A real-time video surveillance system for traffic pre-events detection. *Accident Analysis & Prevention*, *154*, 106019. https://doi.org/10.1016/j.aap.2021.106019

Pramanik, A. R., Sarkar, S., & Sarkar, B. (2022). OSWMI: An objective-subjective weighted method for minimizing inconsistency in multi-criteria decision making. *Computers & Industrial Engineering*, *169*, 108138. https://doi.org/10.1016/j.cie.2022.108138

Polat, H., & Homay, D. M. (2019). Classification of pulmonary CT images by using hybrid 3D-deep convolutional neural network architecture. *Applied Sciences*, *9*(5), 940. https://doi.org/10.3390/app9050940

Punithavathy, K., Sumathi, P., & Ramya, M. M. (2019). Performance evaluation of machine learning techniques in lung cancer classification from PET/CT images. *FME Transactions*, *47*(3), 418-423. https://doi.org/10.5937/fmet1903418p

Qin, R., Wang, Z., Jiang, L., Qiao, K., Hai, J., Chen, J., & Yan, B. (2020). Fine-grained lung cancer classification from PET and CT images based on multidimensional attention mechanism. *Complexity, 2020,* 6153657 (pp. 1-12). https://doi.org/10.1155/2020/6153657

Riquelme, D., & Moulay, A. (2020). Deep learning for lung cancer nodules detection and classification in CT scans. *AI: 1*(1), 28-67. https://doi.org/10.3390/ai1010003

Ruan, J. (2022). Development of deep learning-based automatic scan range setting model for lung cancer screening low-dose CT imaging. *Academic Radiology*, *29*(10), 1541-1551. https://doi.org/10.1016/j.acra.2021.12.001

Saha, A., & Yadav, R. (2023). Study on segmentation and prediction of lung cancer based on machine learning approaches. *International Journal of Experimental Research and Review*, *30*, 1-14. https://doi.org/10.52756/ijerr.2023.v30.001

Sarkar, S., Pramanik, A., Maiti, J., & Reniers, G. (2020). Predicting and analyzing injury severity: A machine learning-based approach using class-imbalanced proactive and reactive data. *Safety Science*, *125*, 104616. https://doi.org/10.1016/j.ssci.2020.104616

Sarkar, S., Vinay, S., Djeddi, C., & Maiti, J. (2021). Text mining-based association rule mining for incident analysis: a case study of a steel plant in India. *In Proceedings: Pattern Recognition and Artificial Intelligence.* 4th Mediterranean Conference, *MedPRAI 2020*, Hammamet, Tunisia, pp. 257-273. https://doi.org/10.1007/978-3-030-71804-6_19

Sarkar, S., Vinay, S., Raj, R., Maiti, J., & Mitra, P. (2019). Application of optimized machine learning techniques for prediction of occupational accidents. *Computers & Operations Research*, *106*, 210-224. https://doi.org/10.1016/j.cor.2018.02.021

Schwyzer, M. (2018). Automated detection of lung cancer at ultralow dose PET/CT by deep neural networks- initial results. *Lung Cancer*, *126*, 170-173. https://doi.org/10.1016/j.lungcan.2018.11.001

Shakeel, P.M., Burhanuddin, M. A., & Mohammad, I. D. (2022). Automatic lung cancer detection from CT image using improved deep neural network and ensemble classifier. *Neural Computing and Applications*, *34*(12), 9579–9592. https://doi.org/10.1007/s00521-020-04842-6

Sharif, M.I. (2020). A comprehensive review on multi-organs tumor detection based on machine learning. *Pattern Recognition Letters*, *131*, 30-37. https://doi.org/10.1016/j.patrec.2019.12.006

Singh, G.A.P., & Gupta, P.K. (2019). Performance analysis of various machine learning-based approaches for detection and classification of lung cancer in humans. *Neural Computing and Applications*, *31*(10), 6863- 6877. https://www.springerprofessional.de/en/performance-analysis-of-various-machine-learning-based-approache/15741460

Thakur, S.K., Singh, D.P., & Choudhary, J. (2020). Lung cancer identification: a review on detection and classification. *Cancer and Metastasis Reviews*, *39*(3), 989-998. https://doi.org/10.1007/s10555-020-09901-x

Toğaçar, M., Burhan, E., & Zafer, C. (2020). Detection of lung cancer on chest CT images using minimum redundancy maximum relevance feature selection method with convolutional neural networks. *Biocybernetics and Biomedical Engineering*, *40*(1), 23-39. https://doi.org/10.1016/j.bbe.2019.11.004

Wang, S. (2019). Predicting EGFR mutation status in lung adenocarcinoma on computed tomography image using deep learning. *European Respiratory Journal*, *53*(3), 1800986. https://doi.org/10.1183/13993003.00986-2018

Yu, K.H. (2020). Reproducible machine learning methods for lung cancer detection using computed tomography images: Algorithm development and validation. *Journal of Medical Internet Research*, *22*(8), e16709. https://doi.org/10.2196/16709

.

How to cite this Article:

N. Sudhir Reddy and V. Khanaa (2023). Diagnosing and categorizing of pulmonary diseases using Deep learning conventional Neural network. *International Journal of Experimental Research and Review*, *31*, 12-22.

DOI : https://doi.org/10.52756/10.52756/ijerr.2023.v31spl.002